

¹ Traits predict forest phenological responses to photoperiod
² more than temperature

³ Deirdre Loughnan¹, Faith A M Jones^{1, 2}, and E M Wolkovich^{1,3,4}

⁴ January 8, 2026

⁵ ¹ Department of Forest and Conservation, Faculty of Forestry, University of British Columbia, 2424
⁶ Main Mall Vancouver, BC Canada V6T 1Z4.

⁷ ² Department of Wildlife, Fish and Environmental Studies, Swedish University of Agricultural Sci-
⁸ ences, 901 83 Umeå, Sweden.

⁹ ³ Arnold Arboretum of Harvard University, 1300 Centre Street, Boston, Massachusetts, USA;

¹⁰ ⁴ Organismic & Evolutionary Biology, Harvard University, 26 Oxford Street, Cambridge, Massachusetts,
¹¹ USA;

¹² Corresponding Author: Deirdre Loughnan deirdre.loughnan@ubc.ca

¹³ Running title: Traits drive photoperiod cues in budburst

¹⁴ **Summary**

¹⁵ As the timing of plant life cycle events—phenology—has shifted with climate change, there is growing
¹⁶ interest to incorporate phenology within plant strategies has received growing interest as phenology
¹⁷ has shifted with climate change. But integrating phenology into to existing spectra (like the leaf
¹⁸ economic spectrum and wood economic spectrum) that consider traits across species has been slow in
¹⁹ part because of high trait variation within-species, which is especially high for phenology. Addressing
²⁰ this requires data on many traits across space and better estimates of phenology, which is less variable
²¹ when determined through experiments that can be used to decompose its environmental drivers (such
²² as chilling and forcing temperatures or photoperiod). Here, working across eight forest communities to
²³ collect *in situ* trait measurements from 1428 individuals of 47 species, we find phenology connects to
²⁴ four major plant functional traits (height, diameter, leaf mass area and nitrogen content) via responses
²⁵ to photoperiod, but not temperature. These results provide insight into the complexity of phenology-
²⁶ trait relationships in relation to cues, as well as novel support for the inclusion of phenology in studies
²⁷ of woody plant growth to accurately forecasts changes in species growth with climate change.

²⁸ **Introduction**

²⁹ Climate change is causing species phenologies—the timing of life history events—to shift, with widespread
³⁰ advances being observed across the tree of life (Parmesan and Yohe, 2003; Hoegh-Guldberg et al., 2018).
³¹ This common phenological fingerprint, however, averages over high variability across species (Thack-
³² eray et al., 2016; Cohen et al., 2018; Kharouba et al., 2018), posing a challenge to accurate forecasts.

³³

39 In plants, species variation can be explained, in part, by differences in growth strategies, which are generally inferred from traits (Violle et al., 2007). Decades of research on plant traits have worked to build
40 predictive models of species responses to their environment (Green et al., 2022), which could explain
41 species-level variability in phenological responses. Phenology, however, has generally been excluded from
42 plant trait research due to its high inter- and intra-specific variability, making it difficult to leverage
43 existing frameworks to explain phenological variation and predictions future changes. Previous studies
44 have found high variation in phenology in observational studies—even for the same species when ob-
45 served over different years or sites (Primack et al., 2009; Chuine et al., 2010), but variation is usually
46 much smaller when calculated from controlled experiments, which suggest that phenological variation
47 can be consistently decomposed into its environmental cues (e.g., temperature and photoperiod Chuine
48 and Cour, 1999; Harrington and Gould, 2015; Flynn and Wolkovich, 2018).

49 Correlations between plant traits, growth strategies, and responses to environments have been synthe-
50 sized into several global frameworks, including the leaf economic spectrum (Wright et al., 2004) and
51 wood economic spectrum (Chave et al., 2009). These frameworks have identified key traits that ex-
52 hibit distinct gradients, ranging from acquisitive strategies—fast growing plants that produce cheaper
53 tissue—to conservative strategies—with plants that invest in long-lived tissue but slower growth rates
54 (Wright et al., 2004; Díaz et al., 2016). In temperate systems, changes in temperature and frost risk in
55 spring can produce gradients in abiotic stress, including frost risk, soil nutrients, and light availability
56 (Sakai and Larcher, 1987; Gotelli and Graves, 1996; Augspurger, 2009), in addition to differences in
57 biotic interactions from herbivory or competition later in the season (Lopez et al., 2008; Wolkovich
58 and Ettinger, 2014). Species that vary in their timing of leafout, should therefore exhibit traits and
59 growth strategies that allow them to tolerate or avoid these abiotic and biotic factors. Leveraging in-
60 sights from predictive models of phenology with these well established trait frameworks could begin to
61 disentangle the environmental cues that shape phenology from those shaped by other trait differences
62 in plant growth strategies.

63

64 To determine whether phenology fits within major functional trait frameworks requires working across
65 within- and between-species variation. Phenological variation is generally observed in natural condi-
66 tions where the environmental cues that trigger many phenological events—primarily temperature and
67 photoperiod (Chuine, 2000; Körner and Basler, 2010)—vary across space and time. But experiments
68 that control for this variation generally find smaller effects across space (??). Within-species variation
69 also occurs across other plant traits (e.g., leaf and wood structure traits), including across latitudinal
70 (Wiemann and Bruce, 2002) and other environmental gradients (Pollock et al., 2012), though gener-
71 ally to a smaller scale compared to phenology. To better understand how phenology and other traits
72 correlate across species will require methods that incorporate spatial variation within species.

73

74 Here, we tested whether phenological variation was aligned with existing trait frameworks using data on
75 spring budburst paired and a suite of traits that capture acquisitive to conservative growth strategies.
76 We decompose the high phenological variation in budburst date by using experiments to estimate
77 three major phenological cues for woody plant budburst: chilling (cool winter temperatures), forcing
78 (warm spring temperatures), and photoperiod. We predict that early spring species will budburst
79 before canopy closure, exhibited as smaller responses to temperature and photoperiod. These species
80 should have traits associated with acquisitive growth, particularly shorter heights, smaller trunk or
81 stem diameters, with lower investment in wood structure and leaf tissue, resulting in low wood specific
82 density, diffuse-porous wood anatomy, and low leaf mass area, but high leaf nitrogen content for a
83 greater photosynthetic potential. In contrast, we predict species with later budburst to predominately
84 include canopy species that express more conservative growth strategies and require more chilling,
85 warmer forcing, and longer photoperiods. These species should incur greater investments in long-lived
86 tissue, with ring-porous wood anatomy, taller heights and greater diameter, denser wood and high
87 leaf mass area, but low leaf nitrogen content. We then used a joint-modeling approach to estimate
88 the relationships between these plant traits and phenological responses to cues, while partitioning the
89 variance from species- and population-level differences.

91 **Materials and Methods**

92 **Field sampling**

93 We combined *in situ* trait data with budburst data from two growth chamber cutting experiments
94 conducted across eastern and western temperate deciduous forests in North America. We collected
95 both suites of data from populations that span a latitudinal gradient of 4-6° for the eastern and
96 western communities respectively. We took trait measurements from across eight populations, of
97 which there were four eastern populations—Harvard Forest, Massachusetts, USA (42.55°N, 72.20°W),
98 White Mountains, New Hampshire, USA (44.11°N, 52.14°W), Second College Grant, New Hampshire,
99 USA (44.79°N, 50.66°W), and St. Hippolyte, Quebec, Canada (45.98°N, 74.01°W), and four western
100 population—E.C. Manning Park (49.06°N, 120.78°W), Sun Peaks (50.88°N, 119.89°W), Alex Fraser
101 Research Forest (52.14°N, 122.14°W), and Smithers (54.78°N, 127.17°W), British Columbia (BC),
102 Canada (Fig. 1). For the two growth chamber studies on budburst phenology, we collected cuttings
103 from the most southern and northern populations in each transect ($n_{pop}=4$).
104

105 **Functional traits**

106 We measured all traits in the summer prior to each growth chamber study (eastern transect: 8-25 June
107 2015, western transect: 29 May to 30 July 2019), following full leafout but before budset. At each
108 population and for each species, we measured a total of five traits from 1-10 healthy adult individuals:
109 height, diameter of the main trunk or stem (hereafter referred to as diameter), wood specific density,
110 leaf mass area, and the percent leaf nitrogen content. We also obtained xylem structure data from the
111 WSL xylem database (Schweingruber and Landolt, 2010) for 72.3% of our species.
112

113 We measured traits in accordance to the methods discussed by Pérez-Harguindeguy et al. (2013).
114 We calculated tree height using trigonometric methods and used a base height of 1.37 m to measure
115 diameter (Magarik et al., 2020). For shrub heights, we measured the distance from the ground to the
116 height of the top foliage and measured stem diameters at approximately 1 cm above ground-level. All
117 stem and leaf samples were kept cool during transport and measurements of leaf area and stem volume
118 taken within 3 and 12 hours of sample collection respectively. To measure wood specific density, we
119 collected a 10 cm sample of branch wood, taken close to the base of the branch at the stem and
120 calculated stem volume using the water displacement method. For our leaf traits, we haphazardly
121 selected and sampled five, fully expanded, and hardened leaves, with no to minimal herbivore damage.
122 We took a high resolution scan of each leaf using a flatbed scanner and estimated leaf area using the
123 ImageJ software (version 2.0.0).

124 **Growth chamber study**

125 For our growth chamber studies, we collected branch cuttings from our highest and lowest latitude
126 populations in each transect, with sampling in our eastern study occurring from 20-28 January 2015
127 and sampling for our western study from 19-28 October 2019. In using cuttings from dormant branches,
128 we are able to experimentally manipulate environmental cues while still approximating whole plant
129 responses in budburst (?). In both studies, we included a total of eight distinct treatments consisting
130 of two levels of chilling, forcing, and photoperiods (Fig. 1). We recorded budburst stages of each
131 sample every 1-3 days for up to four months, defining the day of budburst as the day of budbreak or
132 shoot elongation (denoted as code 07 by Finn et al. (2007)). For a more detailed discussion of study
133 sample collection and methods see Flynn and Wolkovich (2018) for details on our eastern study and
134 Loughnan and Wolkovich (in prep) for details on our western study.

135

136 **Statistical Analysis**

137 Our analysis combined our *in situ* trait data with budburst data from the controlled environment. For
 138 each trait, we developed a joint Bayesian model, in which the relationship between traits and cues
 139 is used to estimate budburst. This statistical approach improves upon previous analyses of multiple
 140 traits, as it allows us to carry through uncertainty between trait and phenology data—and better
 141 partitions the drivers of variation in species phenologies

142 Our joint model consists of two parts. The first is a hierarchical linear model, which partitions the vari-
 143 ation of individual observations (i) of a given trait value (Y_{trait}) to account for the effects of species
 144 (j), population-level differences arising from transects, latitude, as well as the interaction between
 145 transects and latitude ($\text{transect} \cdot \text{latitude}$), and finally, residual variation or ‘measurement error’ (σ_m^2).
 146

147

$$Y_{\text{trait}_{i,j}} \sim \text{Normal}(\mu_{i,j}, \sigma_m^2) \quad (1)$$

$$\mu_{i,j} = \alpha_{\text{grand trait}} + \alpha_{\text{trait}_j} + \beta_{\text{transect}} \times \text{transect} + \quad (2)$$

$$\beta_{\text{latitude}} \times \text{latitude} + \beta_{\text{transect} \cdot \text{latitude}} \times (\text{transect} \cdot \text{latitude}) \quad (3)$$

(4)

148

$$\boldsymbol{\alpha}_{\text{trait}} \begin{bmatrix} \alpha_{\text{trait}_1} \\ \alpha_{\text{trait}_2} \\ \dots \\ \alpha_{\text{trait}_n} \end{bmatrix} \text{ such that } \boldsymbol{\alpha}_{\text{trait}} \sim \text{Normal}(0, \sigma_{\text{trait}}^2) \quad (5)$$

(6)

149 We include transect as a dummy variable (0/1) and latitude as a continuous variable in our model.
 150 We modeled traits using their original units, with the exception of leaf mass area and wood specific
 151 density, which were rescaled by 100 for numeric stability in the model. Our model also includes
 152 partial pooling for species—which controls for variation in the number of trait estimates per species
 153 and trait variability—using these species-level estimates as predictors for each cue ($\beta_{\text{chilling},j}$, $\beta_{\text{forcing},j}$,
 154 $\beta_{\text{photoperiod},j}$).

155

$$\beta_{\text{chilling}_j} = \alpha_{\text{chilling},j} + \beta_{\text{trait.chilling}} \times \alpha_{\text{trait},j} \quad (7)$$

$$\beta_{\text{forcing}_j} = \alpha_{\text{forcing},j} + \beta_{\text{trait.forcing}} \times \alpha_{\text{trait},j}$$

$$\beta_{\text{photoperiod}_j} = \alpha_{\text{photoperiod},j} + \beta_{\text{trait.photoperiod}} \times \alpha_{\text{trait},j}$$

156 In addition to the species-level estimates, the second part of our model estimates the overall effect of
 157 each trait on each cue ($\beta_{\text{trait.chilling}}$, $\beta_{\text{trait.forcing}}$, $\beta_{\text{trait.photoperiod}}$). From this we can estimate how well
 158 traits explain species-level differences—by estimating the the species-level cue variation not explained
 159 by traits ($\alpha_{\text{chilling},j}$, $\alpha_{\text{forcing},j}$, $\alpha_{\text{photoperiod},j}$) and individual species responses to cues (*chilling*, *forcing*,
 160 *photoperiod*, respectively). Finally, our model estimates the residual budburst variation across species
 161 ($Y_{\text{pheno},j}$), observations (σ_d^2), as well as the variation in cues not attributed to the trait (using partial
 162 pooling).

$$Y_{\text{pheno}_{i,j}} \sim \mathcal{N}(\mu_{i,j}, \sigma_d^2) \quad (8)$$

¹⁶³ with

$$\mu_{i,j} = \alpha_{\text{pheno}_j} + \beta_{\text{chilling}_j} \cdot \text{chilling} + \beta_{\text{forcing}_j} \cdot \text{forcing} + \beta_{\text{photoperiod}_j} \cdot \text{photoperiod} \quad (9)$$

¹⁶⁴ where α_{pheno_j} , $\alpha_{\text{chilling}_j}$, $\alpha_{\text{forcing}_j}$, and $\alpha_{\text{photoperiod}_j}$ are elements of the normal random vectors:

$$\boldsymbol{\alpha}_{\text{pheno}} = \begin{bmatrix} \alpha_{\text{pheno}_1} \\ \alpha_{\text{pheno}_2} \\ \dots \\ \alpha_{\text{pheno}_n} \end{bmatrix} \text{ such that } \boldsymbol{\alpha}_{\text{pheno}} \sim \text{Normal}(\mu_{\text{pheno}}, \sigma^2_{\text{pheno}}) \quad (10)$$

$$\boldsymbol{\alpha}_{\text{chilling}} = \begin{bmatrix} \alpha_{\text{chilling}_1} \\ \alpha_{\text{chilling}_2} \\ \dots \\ \alpha_{\text{chilling}_n} \end{bmatrix} \text{ such that } \boldsymbol{\alpha}_{\text{chilling}} \sim \text{Normal}(\mu_{\text{chilling}}, \sigma^2_{\text{chilling}}) \quad (11)$$

$$\boldsymbol{\alpha}_{\text{forcing}} = \begin{bmatrix} \alpha_{\text{forcing}_1} \\ \alpha_{\text{forcing}_2} \\ \dots \\ \alpha_{\text{forcing}_n} \end{bmatrix} \text{ such that } \boldsymbol{\alpha}_{\text{forcing}} \sim \text{Normal}(\mu_{\text{forcing}}, \sigma^2_{\text{forcing}}) \quad (12)$$

$$\boldsymbol{\alpha}_{\text{photoperiod}} = \begin{bmatrix} \alpha_{\text{photoperiod}_1} \\ \alpha_{\text{photoperiod}_2} \\ \dots \\ \alpha_{\text{photoperiod}_n} \end{bmatrix} \text{ such that } \boldsymbol{\alpha}_{\text{photoperiod}} \sim \text{Normal}(\mu_{\text{photoperiod}}, \sigma^2_{\text{photoperiod}}) \quad (13)$$

(14)

¹⁶⁵ We modeled each trait individually, with the exception of ring-porosity, which we compared across
¹⁶⁶ species using the posterior estimates of our wood stem density model, allowing us to account for inher-
¹⁶⁷ ent differences in wood anatomy across species and growth form. We included all three cues (chilling,
¹⁶⁸ forcing, and photoperiod) as continuous variables in our model, as well as all two-way interactions
¹⁶⁹ between cues and between cues and sites. We converted chilling temperatures to total chill portions,
¹⁷⁰ including both the chilling experienced in the field prior to sampling and during the experiment. For
¹⁷¹ this we used local weather station data and the chillR package (v. 0.73.1, Luedeling, 2020). To account
¹⁷² for differences in thermoperiodicity between the two studies (Buonaiuto et al., 2023), we also converted
¹⁷³ forcing temperatures to mean daily temperatures for each treatment. Finally, we *z*-scored each cue
¹⁷⁴ and site using two standard deviations to allow direct comparisons between results across parameters
¹⁷⁵ (Gelman, 2008).

¹⁷⁶

¹⁷⁷ For each model we used trait specific priors that were weakly informative. We validated our choice
¹⁷⁸ of priors using prior predictive checks and confirmed model stability under wider priors. All models
¹⁷⁹ were coded in the Stan programming language for Bayesian models using the rstan package (Stan
¹⁸⁰ Development Team, 2018) in R version 4.3.1 (R Development Core Team, 2017). All models met basic
¹⁸¹ diagnostic checks, including no divergences, high effective sample sizes (n_{eff}) that exceeded 10% of
¹⁸² the number of iterations, and \hat{R} values close to 1. We report our model estimates as the mean values
¹⁸³ with 90% uncertainty intervals (UI), interpreting parameter estimates with intervals that overlap to
¹⁸⁴ be statistically similar to each other and those that include zero to have small effects.

¹⁸⁵

¹⁸⁶ Results

¹⁸⁷ Across our eight populations, we measured 47 species of which 28 were in our eastern transect and
¹⁸⁸ 22 in our western transect. These include species dominant in both the understory and canopy layer,

189 with our eastern community consisting of 13 shrubs and 15 trees, our western community consisting of
190 18 shrubs and 4 trees, and three species that occurred in both transects. In total we measured traits
191 of 1428 unique individuals between the two transects across our five *in situ* traits: height ($n = 1317$),
192 diameter ($n = 1220$), wood stem density ($n = 1359$), leaf mass area ($n = 1345$), leaf nitrogen con-
193 tent ($n = 1351$). Across our two growth chamber studies, we made observations of 4211 samples, with
194 our observations of budburst spanning 82 and 113 days for our eastern and western studies respectfully.
195

196 Most of our traits showed some variation by latitude within each transect, with a strong interactive
197 effect between transect and latitude (Fig. 2). Leaf nitrogen content was the only trait to vary with
198 latitude alone, with low latitude communities on both our eastern and western transects having greater
199 values of leaf nitrogen content than communities at higher latitudes (-0.1, UI: -0.2, 0.0, Table S6). The
200 strongest negative interaction was observed for height (-0.2, UI: -0.4, 0.0), while the strongest positive
201 interaction was observed for leaf mass area (0.5, UI: 0.4, 0.6). Height and wood stem density both ex-
202 hibited negative transect by latitude interactions (-0.2, UI: -0.4, 0.0 for our height model and -0.1, UI:
203 -0.2, -0.1 for our wood stem density model), with woody species in our eastern communities exhibited
204 greater heights and wood stem densities with increasing latitude, but decreasing values with latitude
205 in our western communities (Fig. 2 a and c). In contrast, diameter and leaf mass area both exhibited
206 positive transect by latitude interactions (0.5, UI: 0.1, 0.9 for our diameter model and 0.5, UI: 0.4,
207 0.6 for our leaf mass area model), with plants at higher latitudes having increasing diameters in both
208 our eastern and western communities but decreasing leaf mass areas in our eastern communities and
209 increasing values in our western communities (Fig. 2 b and d). In addition to the differences we found
210 across populations, we also observed considerable differences between individual species, which varied
211 considerably and up to 7 fold for some traits (Fig. 3).

212
213 We found that three of our four traits had a strong relationship with photoperiod, but not always in
214 the direction we predicted. Taller species with larger trunk diameters and leaves with high nitrogen
215 content had larger responses with longer photoperiods (Fig. 3 c, i, o; Tables S2, S3, S6). But, contrary
216 to our expectation, species with denser, high leaf mass area leaves had smaller photoperiod responses,
217 allowing them to potentially budburst under shorter photoperiods (Fig. 3f).

218
219 Temperature cues ($\beta_{\text{trait.chilling}}$ and $\beta_{\text{trait.forcing}}$) exhibited no relationships with individual traits, but
220 by accounting for the effects of leaf or wood traits, we found the importance of our three cues to vary
221 by trait. Chilling (β_{chilling}) was the strongest cue of budburst in our models of height (-13.4 m per
222 standardized chill portions, UI: -17.2, -9.9), diameter (-12.5 cm per standardized chill portions, UI:
223 -16.2, -8.6), wood stem density (-20.9 g/cm³ per standardized chill portions, UI: -33.2, -9.8), and leaf
224 nitrogen content (-35.1 percent per standardized chill portions, UI: -68.1, -4.1), with more chilling
225 advancing budburst. Our model of leaf mass area, however, estimated photoperiod as the strongest
226 cue ($\beta_{\text{photoperiod}}$, -14.0, UI: -23.1, -3.5). After accounting for the effects of traits, only our height and
227 diameter model found all three environmental cues to drive budburst timing (Tables S2, S3). Our
228 models of wood stem density and leaf nitrogen content in turn found temperature cues alone to shape
229 budburst (Tables S4, S6), while our model of leaf mass area found a large response to only photoperiod
230 (Table S5).

231
232 In synthesizing the effects of multiple traits across species, our results can be used to make general-
233 izations across ecologically important groups of species. But only some of our models estimated clear
234 gradients in species timing between trees and shrubs. In particular, we found height to have large
235 correlations between budburst timing and trait values, with earlier estimates of budburst for shrubs
236 (with a mean day of budburst of 10)—especially under greater cues—and later budburst estimates
237 for trees (with a mean day of budburst of 17.3, Fig. S1). Diameter at breast height showed similar
238 trends as estimates from our height model (results not shown). But this was not the case for our two
239 leaf traits. Leaf nitrogen content, for example, showed no distinct separation between shrub and tree
240 functional groups (Fig. S1).

242 Discussion

243 Using our joint modeling approach, we estimated how leaf and wood traits interact with temperature
 244 and photoperiod cues to shape species budburst. We found that photoperiod—often the weakest cue
 245 of budburst (Laube et al., 2014; Zohner et al., 2016; Flynn and Wolkovich, 2018)—was the most im-
 246 portant cue in trait-phenology relationships. In general, we also found trait patterns varied between
 247 our eastern and western transects and with latitude. These spatial differences in trait variation may be
 248 due to differences in the community assemblages, as our western community is more shrub dominated,
 249 with shorter plants with less dense branch wood. This more acquisitive growth strategy suggests these
 250 species are more likely to utilize resources early in the season prior to canopy closure. **Collectively our**
 251 **results provide new insights into the complex tradeoffs between cues and traits and how they differ**
 252 **across large spatial scales.**

253

254 Cues and functional traits

255 We found only partial support for our prediction that species with acquisitive traits—particularly
 256 small trees with low wood density, low leaf mass area, and high leaf nitrogen content—would have
 257 early budburst via smaller temperature and photoperiod responses. We did find species with smaller
 258 heights and diameters to have smaller photoperiod responses. But contrary to our prediction, species
 259 with less dense leaves showed larger responses to photoperiod, while leaves with high nitrogen content
 260 had stronger photoperiod responses. None of our focal traits, however, showed a relationship with tem-
 261 perature (chilling or forcing), which may be due to selection on other physiological processes. Many of
 262 our traits are associated with one or more ecological function (Wright et al., 2004; Pérez-Harguindeguy
 263 et al., 2013; Reich, 2014). In particular, leaf mass area is known to correlate with traits like leaf lifespan
 264 or decomposition rates in addition to light capture (De La Riva et al., 2016). While our results high-
 265 light the ways in which phenology partially aligns with gradients found in established trait frameworks,
 266 they also offer new insight into potential tradeoffs in how varying physiological processes shape species
 267 growth strategies.

268

269 Decades of previous phenology research have found budburst timing to be primarily driven by tem-
 270 perature (chilling and forcing) and weakly by photoperiod (Chuine et al., 2010; Basler and Körner,
 271 2014; Laube et al., 2014). But we found no other traits that correlate with responses to temperature,
 272 **suggesting other cues or biotic interactions** may impact leaf and structural traits in temperate forests.
 273 Leaf mass area also varies with soil moisture, with variation in leaf area allowing plants to reduce
 274 evaporation under dry conditions, and thus selecting for high trait values (De La Riva et al., 2016).
 275 Soil moisture also shapes other phenological events in woody plants, including radial growth phenology
 276 and shoot elongation (Cabon et al., 2020; Peters et al., 2021). If selection by soil moisture is shaping
 277 phenological responses, it may be contributing to the unexpected trends we observed in leaf traits
 278 and the absence of relationships with temperature. **To fully understand how species growth strategies**
 279 **correlate with phenology may thus require additional environmental cues to be considered.**

280

281 The absence of trait-cue relationships between budburst and wood structure and wood stem density
 282 contrasts the findings of previous work linking these traits. Previous studies have found some evidence
 283 that trees with diffuse-porous wood structure leafout earlier than species with ring-porous structures
 284 (Lechowicz, 1984; Panchen et al., 2014; Yin et al., 2016; Osada, 2017; Savage et al., 2022). Using
 285 wood density as alternative measure of wood structure (wood density positively correlates with xylem
 286 resistance to embolism, Hacke et al., 2001), we did not find clear association between our three pheno-
 287 logical cues and xylem structure, despite our data also focusing on species in temperate forests. **Most**

288 of the individuals we measured, however, did have a fairly narrow range of wood specific densities
289 (varying from 0.2 to 0.6 g/cm³) relative to the variation in wood density observed in studies that
290 focus on tropical species or span a more global distribution (?Savage et al., 2022; ?). We did find
291 some variation in wood density across our different sites and with latitude. The larger wood densities
292 we observed at higher latitudes in our eastern transect could be caused by the differences in winter
293 conditions experienced by canopy versus understory species. The canopy tree species that dominate
294 our eastern communities may experience greater horizontal stress from wind and downward pressure
295 from snow, explaining the greater wood densities they exhibit at higher latitudes (MacFarlane and
296 Kane, 2017; MacFarlane, 2020), while species in the shrub dominated western communities experience
297 greater protection from being in the understory.

298
299 In comparing our results with a global meta-analysis of tree trait relationships with budburst cues
300 (Loughnan et al., 2025), we found similar trait-cue relationships for height and leaf mass area. At
301 both the global and continental scales, we found taller tree heights to leafout with longer photoperiods.
302 We also found species with high specific leaf area—which is the inverse of leaf mass area and
303 thus equivalent to low values—exhibited large responses to photoperiod (Loughnan et al., 2025). The
304 consistency of these results, despite the differences in the two spatial scales of these datasets, provides
305 further evidence that alternate underlying mechanisms are shaping how woody species respond to
306 photoperiod cues.

308 Functional traits predict climate change responses

309 Our results offer novel insights into how broader correlations between growth strategies and phenological
310 cues can help predict responses in woody plant communities with climate change. As temperatures
311 rise, particularly at higher latitudes (Hoegh-Guldberg et al., 2018), warmer winter and spring temper-
312 atures may select for earlier budburst in some species. But, since photoperiod will remain fixed, our
313 observed relationships between photoperiod and other traits has the potential to limit species abilities
314 to track temperatures. This could constrain the extent to which some species growth will advance with
315 climate change. Our results suggest that these effects will likely be greater for taller species or canopy
316 trees and species with relatively low leaf mass area. These constraints could have cascading effects
317 on forest communities, as variable species responses to increasing temperatures further alter species
318 growth strategies and their interactions with competitors or herbivores within their communities.

319
320 Our findings of correlations between phenology and other commonly measured traits highlight how
321 accurate forecasts of future changes in phenology can benefit from accounting for the response of other
322 traits to climate change. Across temperature and precipitation gradients, leaf size and shape also
323 change, as species shift to conserve water and mitigate effects of transpiration under higher temper-
324 atures (De La Riva et al., 2016). These changes could impact species photosynthetic potential and
325 ultimately ecosystem services, such as carbon sequestration. While phenological research has focused
326 on forecasting responses to temperature, the correlation of other traits with photoperiod suggests it is
327 also an important cue. By considering the tradeoffs and differences in cues that simultaneously shape
328 plants growth strategies, we can more accurately forecast species phenology and community dynamics
329 under future climates.

331 References

- 332 Augspurger, C. K. 2009. Spring 2007 warmth and frost: phenology, damage and refoliation in a
333 temperate deciduous forest. *Functional Ecology* 23:1031–1039.

- 334 Basler, D., and C. Körner. 2014. Photoperiod and temperature responses of bud swelling and bud
335 burst in four temperate forest tree species. *Tree Physiology* 34:377–388.
- 336 Buonaiuto, D. M., E. M. Wolkovich, and M. J. Donahue. 2023. Experimental designs for testing the
337 interactive effects of temperature and light in ecology : The problem of periodicity. *Functional
338 Ecology* 37:1747–1756.
- 339 Cabon, A., L. Fernández-de-Uña, G. Gea-Izquierdo, F. C. Meinzer, D. R. Woodruff, J. Martínez-
340 Vilalta, and M. De Cáceres. 2020. Water potential control of turgor-driven tracheid enlargement in
341 Scots pine at its xeric distribution edge. *New Phytologist* 225:209–221.
- 342 Chave, J., D. Coomes, S. Jansen, S. L. Lewis, N. G. Swenson, and A. E. Zanne. 2009. Towards a
343 worldwide wood economics spectrum. *Ecology Letters* 12:351–366.
- 344 Chuine, I. 2000. A unified model for budburst of trees. *Journal of Theoretical Biology* 207:337–347.
- 345 Chuine, I., and P. Cour. 1999. Climatic determinants of budburst seasonality in four temperate-zone
346 tree species. *New Phytologist* 143:339–349.
- 347 Chuine, I., X. Morin, and H. Bugmann. 2010. Warming, photoperiods, and tree phenology. *Science*
348 329:277–278.
- 349 Cohen, J. M., M. J. Lajeunesse, and J. R. Rohr. 2018. A global synthesis of animal phenological
350 responses to climate change. *Nature Climate Change* 8:224–228.
- 351 De La Riva, E. G., M. Olmo, H. Poorter, J. L. Uberta, and R. Villar. 2016. Leaf Mass per Area (LMA)
352 and Its Relationship with Leaf Structure and Anatomy in 34 Mediterranean Woody Species along a
353 Water Availability Gradient. *PLOS ONE* 11:e0148788.
- 354 Diaz, S., J. Kattge, J. H. C. Cornelissen, I. J. Wright, S. Lavorel, S. Dray, B. Reu, M. Kleyer, C. Wirth,
355 I. Colin Prentice, E. Garnier, G. Bönisch, M. Westoby, H. Poorter, P. B. Reich, A. T. Moles, J. Dickie,
356 A. N. Gillison, A. E. Zanne, J. Chave, S. Joseph Wright, S. N. Sheremet'ev, H. Jactel, C. Baraloto,
357 B. Cerabolini, S. Pierce, B. Shipley, D. Kirkup, F. Casanoves, J. S. Joswig, A. Günther, V. Falcuk,
358 N. Rüger, M. D. Mahecha, and L. D. Gorné. 2016. The global spectrum of plant form and function.
359 *Nature* 529:167–171.
- 360 Finn, G. A., A. E. Straszewski, and V. Peterson. 2007. A general growth stage key for describing trees
361 and woody plants. *Annals of Applied Biology* 151:127–131.
- 362 Flynn, D. F. B., and E. M. Wolkovich. 2018. Temperature and photoperiod drive spring phenology
363 across all species in a temperate forest community. *New Phytologist* 219:1353–1362.
- 364 Gelman, A. 2008. Scaling regression inputs by dividing by two standard deviations. *Statistics in
365 Medicine* 27:2865–2873.
- 366 Gotelli, N. J., and G. R. Graves. 1996. The temporal niche. Pages 95–112 in Null Models In Ecology.
367 Smithsonian Institution Press, Washington, D. C.
- 368 Green, S. J., C. B. Brookson, N. A. Hardy, and L. B. Crowder. 2022. Trait-based approaches to
369 global change ecology: moving from description to prediction. *Proceedings of the Royal Society B:
370 Biological Sciences* 289:1–10.
- 371 Hacke, U. G., J. S. Sperry, W. T. Pockman, S. D. Davis, and K. A. McCulloh. 2001. Trends in wood
372 density and structure are linked to prevention of xylem implosion by negative pressure. *Oecologia*
373 126:457–461.
- 374 Harrington, C. A., and P. J. Gould. 2015. Tradeoffs between chilling and forcing in satisfying dormancy
375 requirements for Pacific Northwest tree species. *Frontiers in Plant Science* 6:1–12.

- 376 Hoegh-Guldberg, O., D. Jacob, M. Taylor, M. Bind, S. Brown, I. Camilloni, A. Diedhiou, R. Djalante,
377 K. Ebi, F. Engelbrecht, J. Guiot, Y. Hijioka, S. Mehrotra, A. Payne, S. Seneviratne, A. Thomas,
378 R. Warren, and G. Zhou. 2018. Impacts of 1.5 °C Global Warming on Natural and Human Systems.
379 In: Global Warming of 1.5 °C. An IPCC Special Report on the impacts of global warming of 1.5 °C
380 above pre-industrial levels and related global greenhouse gas emission pathways, in the context of .
381 Tech. rep., Cambridge University Press, Cambridge, UK and New York, NY, USA.
- 382 Kharouba, H. M., J. Ehrlén, A. Gelman, K. Bolmgren, J. M. Allen, S. E. Travers, and E. M. Wolkovich.
383 2018. Global shifts in the phenological synchrony of species interactions over recent decades. Pro-
384 ceedings of the National Academy of Sciences 115:5211–5216.
- 385 Körner, C., and D. Basler. 2010. Phenology Under Global Warming. Science 327:1461–1463.
- 386 Laube, J., T. H. Sparks, N. Estrella, J. Höfler, D. P. Ankerst, and A. Menzel. 2014. Chilling outweighs
387 photoperiod in preventing precocious spring development. Global Change Biology 20:170–182.
- 388 Lechowicz, M. J. 1984. Why Do Temperate Deciduous Trees Leaf Out at Different Times? Adaptation
389 and Ecology of Forest Communities. The American Naturalist 124:821–842.
- 390 Lopez, O. R., K. Farris-Lopez, R. A. Montgomery, and T. J. Givnish. 2008. Leaf phenology in relation
391 to canopy closure in southern Appalachian trees. American Journal of Botany 95:1395–1407.
- 392 Loughnan, D., F. A. Jones, G. Legault, C. J. Chamberlain, D. M. Buonaiuto, A. K. Ettinger, M. Gar-
393 ner, D. S. Sodhi, and E. M. Wolkovich. 2025. Budburst timing within a functional trait framework.
394 Journal of Ecology 00:1–12.
- 395 Loughnan, D., and E. M. Wolkovich. in prep. Temporal assembly of woody plant communities shaped
396 equally by evolutionary history as by current environments .
- 397 Luedeling, E. 2020. chillR: Statistical Methods for Phenology Analysis in Temperate Fruit Trees.
398 <https://CRAN.R-project.org/package=chillR>.
- 399 MacFarlane, D. W. 2020. Functional Relationships Between Branch and Stem Wood Density for
400 Temperate Tree Species in North America. Frontiers in Forests and Global Change 3.
- 401 MacFarlane, D. W., and B. Kane. 2017. Neighbour effects on tree architecture: functional trade-offs
402 balancing crown competitiveness with wind resistance. Functional Ecology 31:1624–1636.
- 403 Magarik, Y. A., L. A. Roman, and J. G. Henning. 2020. How should we measure the dbh of multi-
404 stemmed urban trees? Urban Forestry & Urban Greening 47:1–11.
- 405 Osada, N. 2017. Relationships between the timing of budburst, plant traits, and distribution of 24
406 coexisting woody species in a warm-temperate forest in Japan. American Journal of Botany 104:550–
407 558.
- 408 Panchen, Z. A., R. B. Primack, B. Nordt, E. R. Ellwood, A. Stevens, S. S. Renner, C. G. Willis,
409 R. Fahey, A. Whittemore, Y. Du, and C. C. Davis. 2014. Leaf out times of temperate woody
410 plants are related to phylogeny, deciduousness, growth habit and wood anatomy. New Phytologist
411 203:1208–1219.
- 412 Parmesan, C., and G. Yohe. 2003. A globally coherent fingerprint of climate change impacts across
413 natural systems. Nature 421:37–42.
- 414 Pérez-Harguindeguy, N., S. Díaz, E. Garnier, S. Lavorel, H. Poorter, P. Jaureguiberry, M. S. Bret-
415 Harte, W. K. Cornwell, J. M. Craine, D. E. Gurvich, C. Urcelay, E. J. Veneklaas, P. B. Reich,
416 L. Poorter, I. J. Wright, P. Ray, L. Enrico, J. G. Pausas, A. C. de Vos, N. Buchmann, G. Funes,
417 F. Quétier, J. G. Hodgson, K. Thompson, H. D. Morgan, H. ter Steege, M. G. A. van der Heijden,

- 418 L. Sack, B. Blonder, P. Poschlod, M. V. Vaineretti, G. Conti, A. C. Staver, S. Aquino, and J. H. C.
419 Cornelissen. 2013. New handbook for standardized measurement of plant functional traits worldwide.
420 Australian Journal of Botany 61:167–234.
- 421 Peters, R. L., K. Steppe, H. E. Cuny, D. J. De Pauw, D. C. Frank, M. Schaub, C. B. Rathgeber,
422 A. Cabon, and P. Fonti. 2021. Turgor – a limiting factor for radial growth in mature conifers along
423 an elevational gradient. New Phytologist 229:213–229.
- 424 Pollock, L. J., W. K. Morris, and P. A. Vesk. 2012. The role of functional traits in species distributions
425 revealed through a hierarchical model. Ecography 35:716–725.
- 426 Primack, R. B., I. Ibáñez, H. Higuchi, S. D. Lee, A. J. Miller-Rushing, A. M. Wilson, and J. A. Silan-
427 der. 2009. Spatial and interspecific variability in phenological responses to warming temperatures.
428 Biological Conservation 142:2569–2577.
- 429 R Development Core Team. 2017. R: A language and environment for statistical computing.
- 430 Reich, P. B. 2014. The world-wide ‘fast–slow’ plant economics spectrum: a traits manifesto. Journal
431 of Ecology 102:275–301.
- 432 Sakai, A., and W. Larcher. 1987. Frost Survival of Plants: Responses and adaptation to freezing stress.
433 Springer-Verlag, Berlin, Heidelberg.
- 434 Savage, J. A., T. Kiecker, N. McMann, D. Park, M. Rothendler, and K. Mosher. 2022. Leaf out time
435 correlates with wood anatomy across large geographic scales and within local communities. New
436 Phytologist 235:953–964.
- 437 Schweingruber, F., and W. Landolt. 2010. The xylem database.
- 438 Stan Development Team. 2018. RStan: the R interface to Stan. R package version 2.17.3.
- 439 Thackeray, S. J., P. A. Henrys, D. Hemming, J. R. Bell, M. S. Botham, S. Burthe, P. Helaouet,
440 D. G. Johns, I. D. Jones, D. I. Leech, E. B. MacKay, D. Massimino, S. Atkinson, P. J. Bacon,
441 T. M. Brereton, L. Carvalho, T. H. Clutton-Brock, C. Duck, M. Edwards, J. M. Elliott, S. J. Hall,
442 R. Harrington, J. W. Pearce-Higgins, T. T. Høye, L. E. Kruuk, J. M. Pemberton, T. H. Sparks,
443 P. M. Thompson, I. White, I. J. Winfield, and S. Wanless. 2016. Phenological sensitivity to climate
444 across taxa and trophic levels. Nature 535:241–245.
- 445 Vialle, C., M. Navas, D. Vile, E. Kazakou, C. Fortunel, I. Hummel, and E. Garnier. 2007. Let the
446 concept of trait be functional! Oikos 116:882–892.
- 447 Wiemann, M. C., and W. G. Bruce. 2002. Geographic variation in wood specific gravity: effects of
448 latitude, temperature, and precipitation. Wood and Fiber Science 34:96–107.
- 449 Wolkovich, E. M., and A. K. Ettinger. 2014. Back to the future for plant phenology research. New
450 Phytologist 203:1021–1024.
- 451 Wright, I. J., M. Westoby, P. B. Reich, J. Oleksyn, D. D. Ackerly, Z. Baruch, F. Bongers, J. Cavender-
452 Bares, T. Chapin, J. H. C. Cornelissen, M. Diemer, J. Flexas, J. Gulias, E. Garnier, M. L. Navas,
453 C. Roumet, P. K. Groom, B. B. Lamont, K. Hikosaka, T. Lee, W. Lee, C. Lusk, J. J. Midgley,
454 Ü. Niinemets, H. Osada, H. Poorter, P. Pool, E. J. Veneklaas, L. Prior, V. I. Pyankov, S. C.
455 Thomas, M. G. Tjoelker, and R. Villar. 2004. The worldwide leaf economics spectrum. Nature
456 428:821–827.
- 457 Yin, J., J. D. Fridley, M. S. Smith, and T. L. Bauerle. 2016. Xylem vessel traits predict the leaf
458 phenology of native and non-native understorey species of temperate deciduous forests. Functional
459 Ecology 30:206–214.

- ⁴⁶⁰ Zohner, C. M., B. M. Benito, J.-C. Svenning, and S. S. Renner. 2016. Day length unlikely to constrain
⁴⁶¹ climate-driven shifts in leaf-out times of northern woody plants. *Nature Climate Change* 6:1120–
⁴⁶² 1123.

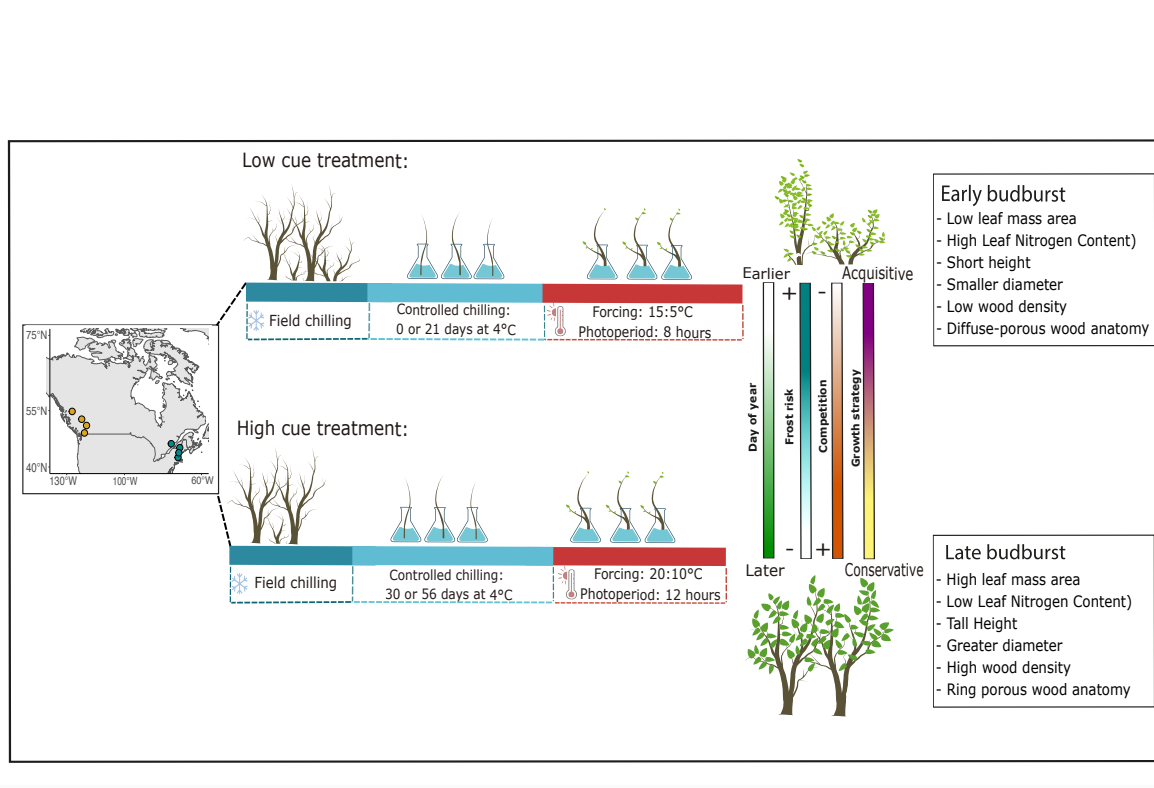


Figure 1: We collected traits data and branch cuttings from plants growing within eight sites, across two transects in eastern and western North America. Cuttings were used in two controlled environment studies in which we applied an high and low chilling, forcing, and photoperiod treatments respectively and recorded the day of budburst of each individual. Using our paired *in situ* trait and experimental budburst data, we tested whether earlier budbursting species exhibited traits associated with more acquisitive growth strategies and smaller responses to cues and later budbursting species a more conservative growth strategy and larger responses to cues.

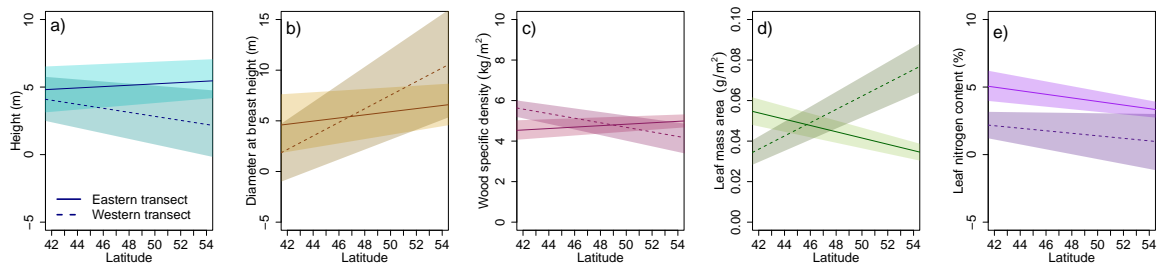


Figure 2: We found a. height, b. diameter, c. branch stem density, and d. leaf mass area to all experience a strong interaction between latitude and transect, e. while leaf nitrogen content showed a strong effect of latitude alone.

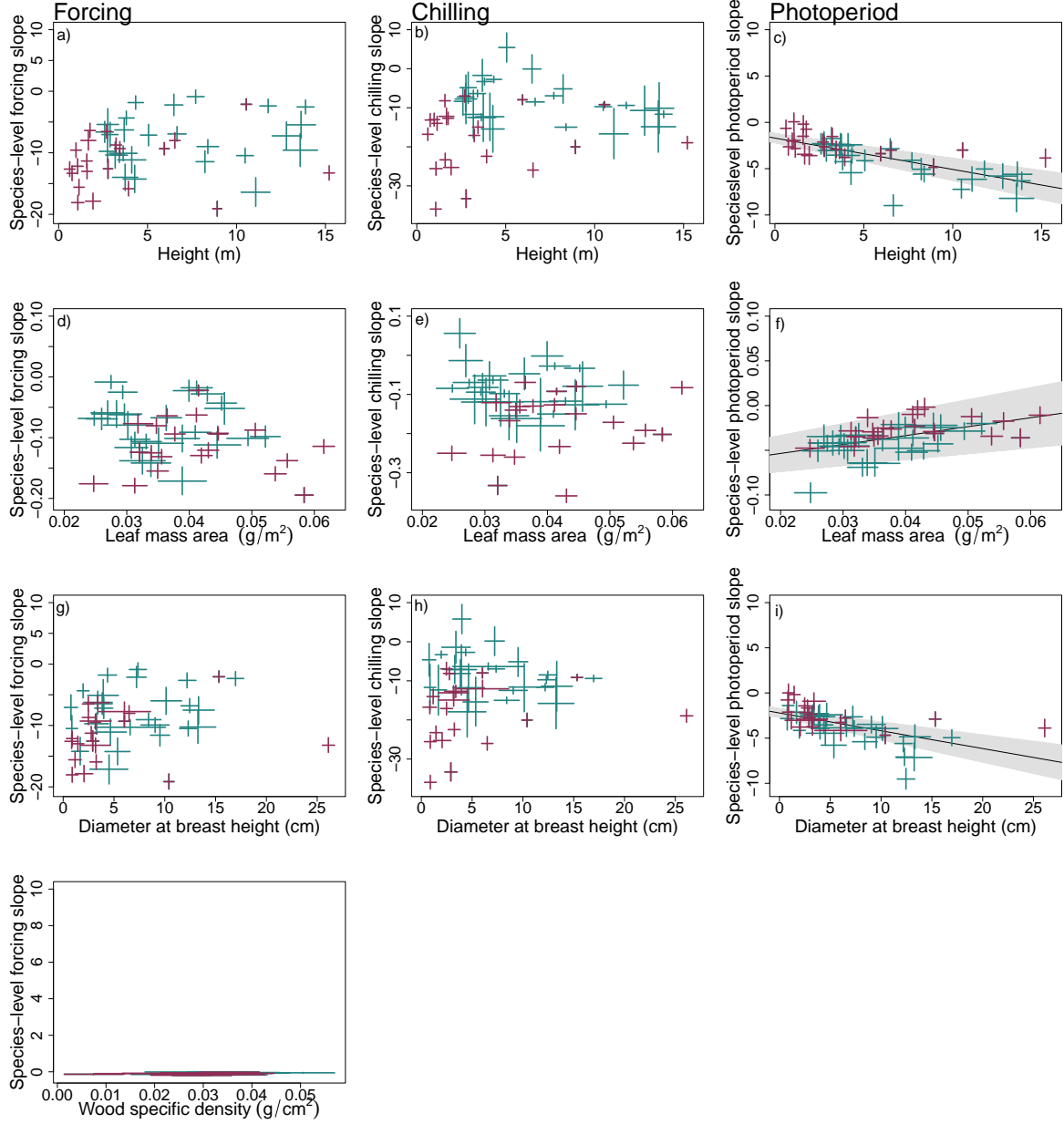


Figure 3: Relationships between species traits and cue responses showed considerable variation across a-c. height, d-f. leaf mass area, g-i. diameter, j-l. wood specific density, and m-o. the leaf nitrogen content. Point colours representing different species groups, with tree species shown in red and shrub species in blue. Crosses depict the 50% uncertainty interval of the model estimates of species trait values and estimated responses to cues. Grey bands depict large relationships between a trait and cue, representing the 90% uncertainty interval, and black lines the mean response.

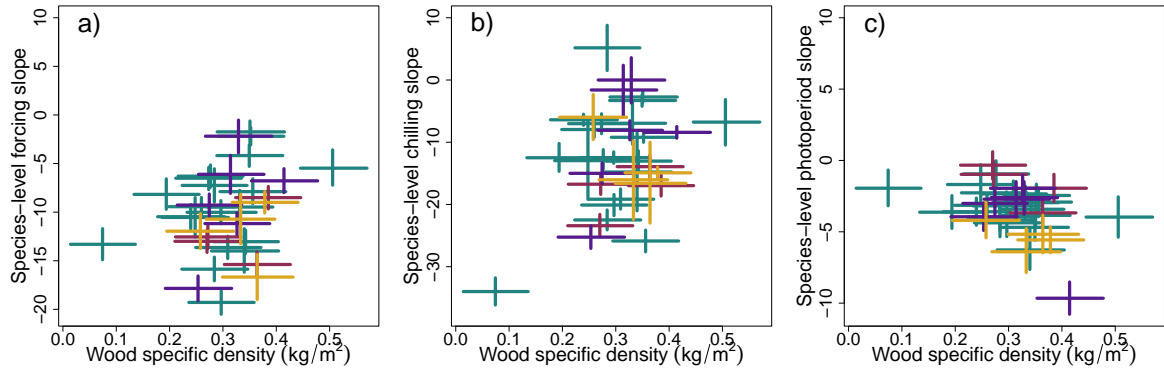


Figure 4: Despite previous studies finding relationships between leaf out timing and species wood xylem structures, we did not find clear differences in species-level estimates of cue responses with wood structure or relative to their wood specific densities. Each cross represents the 50% uncertainty interval of **a.** forcing, **b.** chilling, and **c.** photoperiod responses and wood specific density, with colors depicting different types of wood structure. The lowest wood specific density was observed in *Sambucus racemosa* and the highest wood specific density for *Viburnum lantanoides*.